*Int. J. Electrochem. Sci.*, 11 **(2016)** 665 - 674

International Journal of
ELECTROCHEMICAL
SCIENCE
www.electrochemsci.org

# Study on Nitrogen-Doped Carbon Nanotubes for Vanadium Redox Flow Battery Application

*Jinbin Lin*[1], *Yesheng Shang*[1], *Xiujing Lin*[1], *Linlin Yang*[1,2,*], *Aishui Yu*[1,*]

[1] Department of Chemistry, Collaborative Innovation Center of Chemistry for Energy Materials, Shanghai Key Laboratory of Molecular Catalysis and Innovative Materials, Institute of New Energy, Fudan University, Shanghai 200438, China
[2] Shanghai Electric Group Co., Ltd. Central Academe, Shanghai 200070, China
[*]E-mail: asyu@fudan.edu.cn; yanglinlinzh@163.com

*Received:* 27 May 2015 / *Accepted:* 17 June 2015 / *Published:* 1 December 2015

Nitrogen doped carbon nanotubes(N-CNTs) have been synthesized on carbon felt (N-CNT/CF) with chemical vapor deposition method by utilizing decomposition of melamine in the presence of ferrocene. The as-prepared N-CNT/CF composite was investigated as positive electrodes for vanadium redox flow batteries(VRBs). The microporous nanotube networks consisting of N-CNTs with higher surface area can increase the electrochemical reactive area, which means that N-CNT/CF can generate more active sites for $VO^{2+}/VO_2^+$ redox couple. The charge-discharge test of the full battery with N-CNT/CF as positive electrode showed that the N-CNT/CF electrode gave better battery performance in terms of rate capability and polarization.

**Keywords:** Nitrogen doped carbon nanotubes; carbon felt; Vanadium redox flow batteries; $VO^{2+}/VO_2^+$ redox couple

## 1. INTRODUCTION

With the rapid development of renewable energy(solar energy, wind energy, tidal energy, etc), energy storage system has become more and more attractive due to the intermittence of the renewable energy. Vanadium redox flow batteries (VRBs) have emerged as a kind of very promising options for large-scale energy storage device for its low cost, long lifetime and flexible design and so on. Most importantly, VRBs which employ the same element (vanadium) in the positive and negative electrolytes can reduce the problem of membrane cross contamination[1]. The electrode, which is generally carbon-based materials, plays very important role in VRBs. Among carbon-based materials， carbon felt(CF) is widely used as the electrode of VRBs, due to its low cost, high

conductivity, high surface area and so on. However, the kinetic reversibility and electrochemical activity of CF are poor[2-3]. It is effective to address this problem by introducing an electrocatalyst on the surface of carbon fibers in the CF. Carbon nanotubes(CNTs) are widely applied to batteries, supercapacitors and $H_2$ storage and so on, owing to their prominent physical and chemical properties[4-7]. Recently nitrogen-doped carbon nanotubes(N-CNTs) are considered as excellent electrode material in the batteries field, such as fuel batteries[8], lithium ions batteries[9] and $H_2$ storage[10], due to the bamboo-shaped structure of N-CNTs providing high surface areas, high density of defects and active sites[11]. Therefore, N-CNTs modified CF is of great significance to improve the battery performance.

In this paper, we used Melamine as the precursor of the nitrogen and carbon source to synthesize N-CNTs via the chemical vapor deposition method(CVD) and studied the catalytic effect of N-CNTs on the electrochemical performance of VRBs.

## 2. EXPERIMENTAL

### *2.1 Preparation*

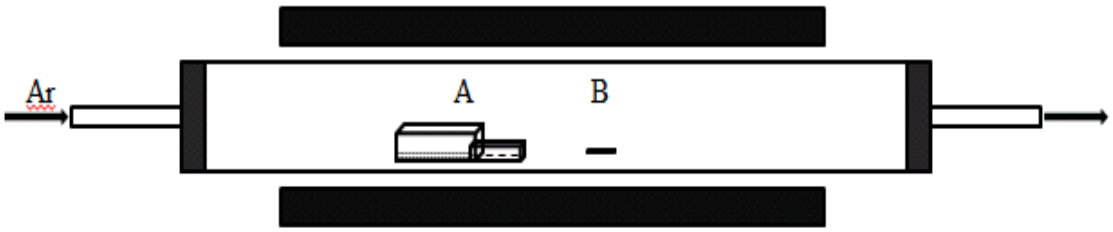


**Figure 1.** Schematic diagram of the synthesis apparatus

In the experiment, N-CNTs were synthesized on the carbon felt by CVD. Ferrocene and melamine were respectively used as the catalyst precursor and the carbon and nitrogen source. Carbon felt (7.5 cm×8.5 cm) which was treated with concentrated nitric acid for 20 h at room temperature was used as a supporter of the N-CNTs growth. The layout is similar to the synthesis one of Y. Chai, et al[12].As shown in Fig. 1, there is a corundum tube(diameter: 8 cm) in a furnace. 11.0210 g of Melamine and 0.7650 g of ferrocene were placed in the big and small porcelain boat, respectively. The place labeled as A laid up a big porcelain boat and a small one and the place labeled as B laid up a piece of CF. The distance between the big boat and the CF was 15 cm.

At first, the air of the corundum tube was removed by introducing Argon (99.999% ) at a flow rate of 1L/min for 30 min. Then the tube was heated to 850 ˚C at the rate of 10 ˚C /min. The precursors evaporated were carried by Argon into the place labeled as B where the pyrolysis of the precursors and the synthesis of N-CNTs occurred. After 60 min, the system cooled down to room temperature in an Argon atmosphere.

*2.2 Physical Characterization*

The sample was characterized by field-emission scanning electron microscopy(FE-SEM, Hitachi S-4800A) and transmission electron microscopy(TEM, JEM-2100F). XPS measurements were performed using a Kratos Axis Ultra X-ray photoelectron spectrometer (Al Ka source).

*2.3 Electrochemical Measurement*

Electrochemical performance of the sample was characterized by cyclic voltammetry (CV) on an electrochemical workstation at room temperature, utilizing a three-electrode electrochemical cell. A piece of Pt and $Hg/Hg_2Cl_2$ electrode were used as the counter and reference electrodes, respectively. The working electrode was the gold wire linked N-CNTs modified CF(0.3 cm×0.4 cm) composite(N-CNT/CF). CV measurements were carried out in the solution of 0.9 M V(III) +0.8 M V(IV) + 2 M $H_2SO_4$ at scan rate of 5 mV/s in the voltage range from -1.0 V to 0 V and 0 V to 1.4 V. In comparison, the acid treated CF was used as the working electrode.

The charge-discharge test was performed by a flow VRB on the BPChecker2000.V3 System(KIKUSUI ELECTRONICS CORP.). The positive and negative electrode were N-CNT/CF(6 cm×8 cm) and the CF(6 cm×8 cm), respectively. The membrane of the VRB was the Nafion 212 membrane (Dupont, USA). The peristaltic pump (Baoding Longer Precision Pump Co., Ltd.) used was BT100-1L pump. Both the positive and negative electrolyte were 50 mL of 0.9 M V(III) +0.8 M V(IV)+2 M $H_2SO_4$. At the constant current density of 40 $mA/cm^2$, the VRB was charged to 1.65 V and discharged to 0.8 V. Compared with N-CNT/CF, the CF treated for 20h by concentrated nitric acid was used as positive electrode.

## 3. RESULTS AND DISCUSSION

Fig. 2a and 2b show the scanning electron microscopy (SEM) image of the untreated CF and acid treated CF, respectively. The carbon fibers in the untreated CF showed the comparatively smooth surface. In comparison, deep grooves could be seen on carbon fibers in the acid treated CF, which indicated the corrosion on carbon fibers after the acid treatment. As a consequence, more carriers of the catalyst particles appeared on carbon fibers, which led to the dense growth of N-CNTs. Therefore ， N-CNTs were synthesized on carbon fibers in the acid treated CF. As demonstrated in Fig. 2c, the dispersal of N-CNTs on carbon fibers was relatively uniform and microporous nanotube networks have been grown on carbon fibers, which can increase the electrochemical reactive area during the periods of charge and discharge of the battery, resulting in prominently enhanced battery performance . The formation of tubular structure has been proved in TEM images. Fig. 2d shows that N-CNTs were twisted each other and the diameter of N-CNTs was 20~40 nm. Compared with carbon fibers(~10 μm), N-CNTs have a high surface area which favors the electrocatalytic reactions. Fig. 2e displays that N-CNTs were a bamboo-like structure with transverse carbon bridges, as previously reported[13-14]. Compared with the length of C−C bond, the length of C−N one is shorter, leading to the curving of

basal planes forming the bamboo-like structure[15]. A more interesting thing is that some N-CNTs with open-mouth end can be seen, which suggests that it is possible that the open-mouth growth mechanism exists during the growth of N-CNTs. What's more, it is found that particles are on the top or packed in the middle of N-CNTs. The particles may be Fe, iron carbide or amorphous carbon. From Fig. 2f, a multi-walled tube can be clearly seen with a rough surface. Moreover, a piece of N-CNT has thick and irregular walls. It is attributed to the pyridinc N, since the pyridinc N makes the shape of nanotubes into an ellipse.

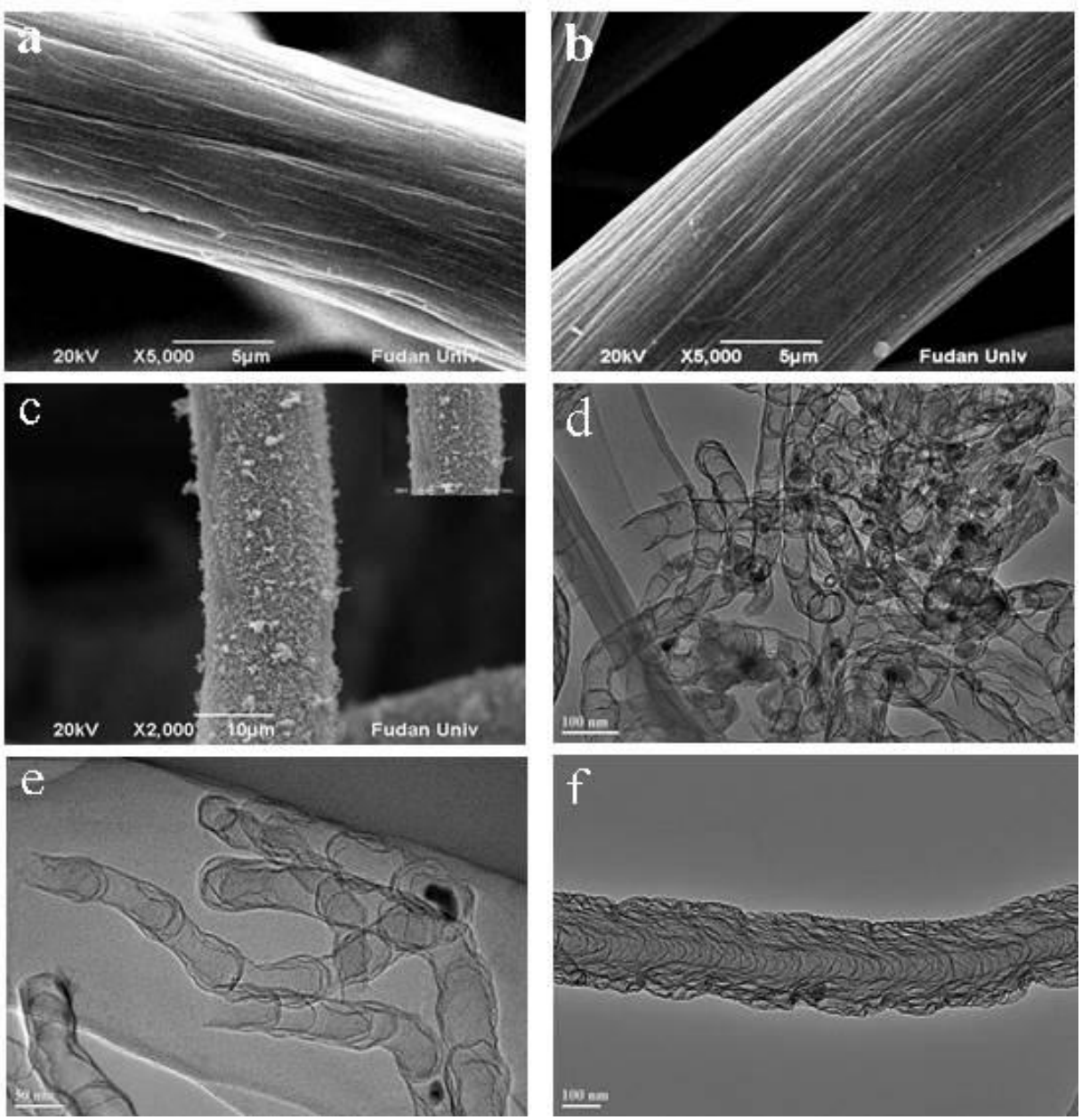


**Figure 2.** SEM images of (a) the untreated CF, (b) the acid treated CF and (c)N-CNTs grown on carbon fibers in the acid treated CF. TEM images of N-CNTs grown on the acid treated CF: (d) low magnification TEM image, (e) high magnification TEM image (f) high magnification TEM image of one N-CNT.

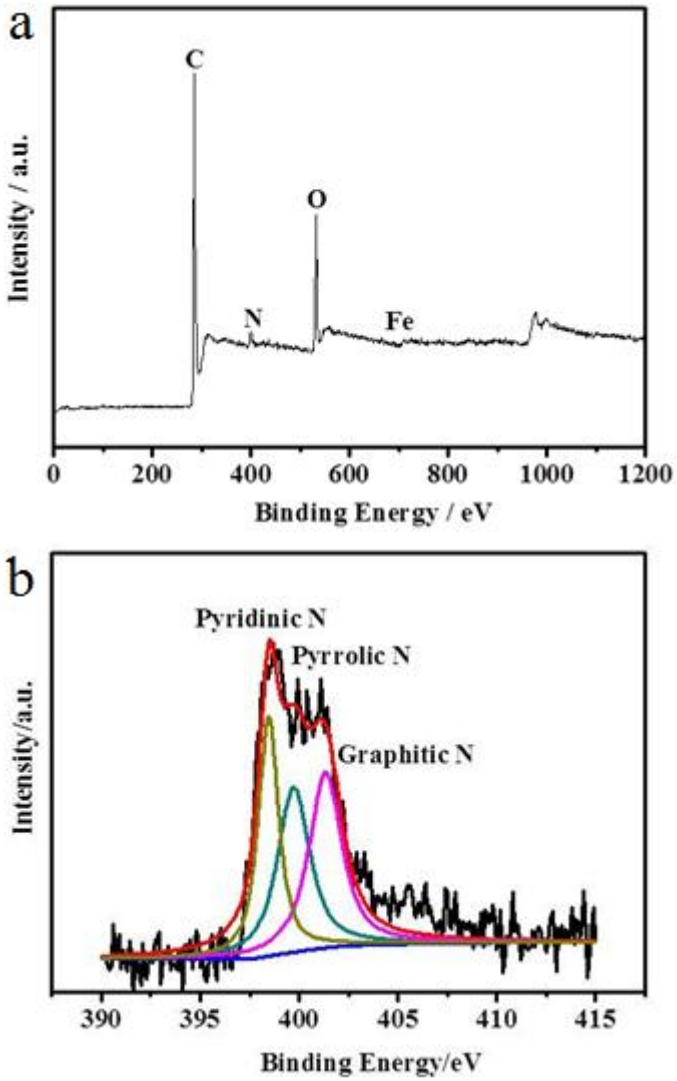


**Figure 3.** (a) Survey XPS spectrum and (b) N1s XPS spectrum of the N-CNT

XPS analysis is used to characterize the content and types of nitrogen incorporated in the N-CNTs. Fig. 3a shows the existence of C, N, O and a small amount of Fe. The nitrogen content, defined as atomic percent of N relative to the total of C and N, is estimated by the ratio between the area of N peak and the total of C and N peaks[11]. Therefore, 4.2 % of the nitrogen content can be figured out. The oxygen species seen from Fig. 3a may be attributed to the adsorption of the N-CNTs surface to the oxygen. To the removal of a small amount of Fe, the sample is impregnated in the HCl solution. As shown in Fig. 3b, the N peak was deconvoluted into three subpeaks to understand the types of nitrogen. Three subpeaks at 398.44 eV, 399.72 eV and 401.33 eV correspond to pyridinic N , pyrrolic N and graphitic N, respectively. From Fig. 3b, it was observed that pyridinic N is the majoringredient. It has been proposed that pyridinic N can deform the structure of N-CNTs, resulting in generating the defect sites. It has been proved that the defect sites can increase the adsorption of oxygen in fuel cells[16-17], thus improving the electrocatalytic activity of N-doped carbon samples. Consequently,

pyridinic N which is dominant in the type of nitrogen can electrochemically enhance the active of N-CNTs.

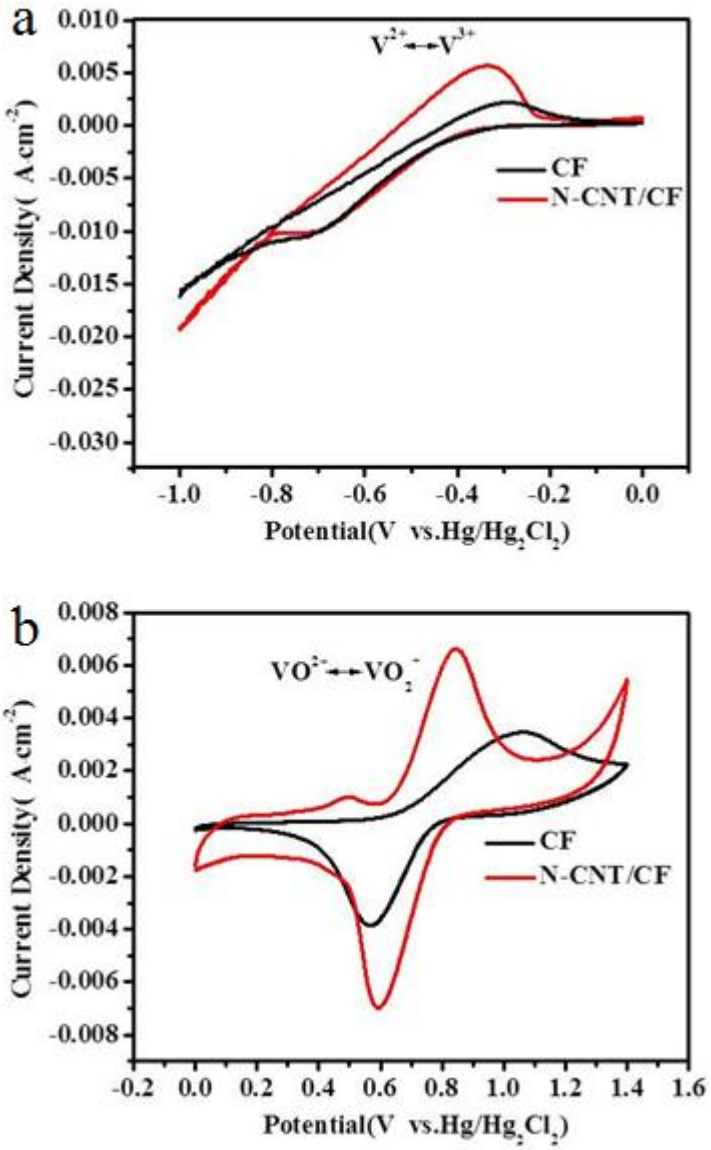


**Figure 4.** CV curves of the CF and N-CNT/CF electrode reaction corresponding to (a) $V^{2+}/V^{3+}$ redox couple and (b) $VO^{2+}/VO_2^+$ redox couple in 0.9 M V(III) +0.8 M V(IV) + 2 M $H_2SO_4$ at scan rate of 5 mV/s, respectively.

Cyclic voltammetry was used for evaluating the catalytic effect of N-CNTs on the $V^{2+}/V^{3+}$ and $VO^{2+}/VO_2^+$ redox couple. Fig. 4a presents CV curves of the CF and N-CNT/CF electrode reaction corresponding to $V^{2+}/V^{3+}$. The anodic peak of the N-CNT/CF electrode showed a negative shift to -0.33 V. And the cathodic peak of the N-CNT/CF electrode appear at -0.73 V, which displays more prominent than that of the CF one. This result reveals that the N-CNT/CF electrode has the better performance in negative half-cell than the CF one, owing to suppressing hydrogen evolution, as

previously reported[18-19]. As for the positive electrode associated with $VO^{2+}/VO_2^+$ (Fig. 4b), the onset potential in the anodic and cathodic reaction showed a negative shift to 0.85 V and a positive shift to 0.60 V, respectively, which would be in favor of electron transfer kinetics and beneficial to increase energy storage efficiency. This is due to a lower applied voltage for the VRB, which implies the redox reaction of vanadium ions on the N-CNT/CF electrode can react more easily than that on the CF electrode[20]. The wettability of CF was improved due to the introduction of N-CNTs.Therefore, the N-CNT/CF can be quickly wetted in the electrolyte, but it takes long time to wet the CF under ultrasonication. Owing to the improvement of the wettability, the concentration of vanadium ions could be increased on the surface of CF, leading to higher peak current[21]. Compared with the CF electrode, the anodic and cathodic peak current density in the N-CNT/CF one were obviously improved, which is attributed to the improvement of the wettability on the N-CNT/CF electrode. Therefore, the N-CNT/CF exhibits better electrocatalytic activity than the CF. The reversibility of redox reaction can be estimated by the ratio of the anodic peak current density and the cathodic peak current density($I_{pa}/I_{pc}$), which is 0.98 and 1.08 for the N-CNT/CF and CF as the positive electrode, respectively, indicating that the reversibility on the N-CNT/CF electrode is greatly enhanced compared with that on the CF one.

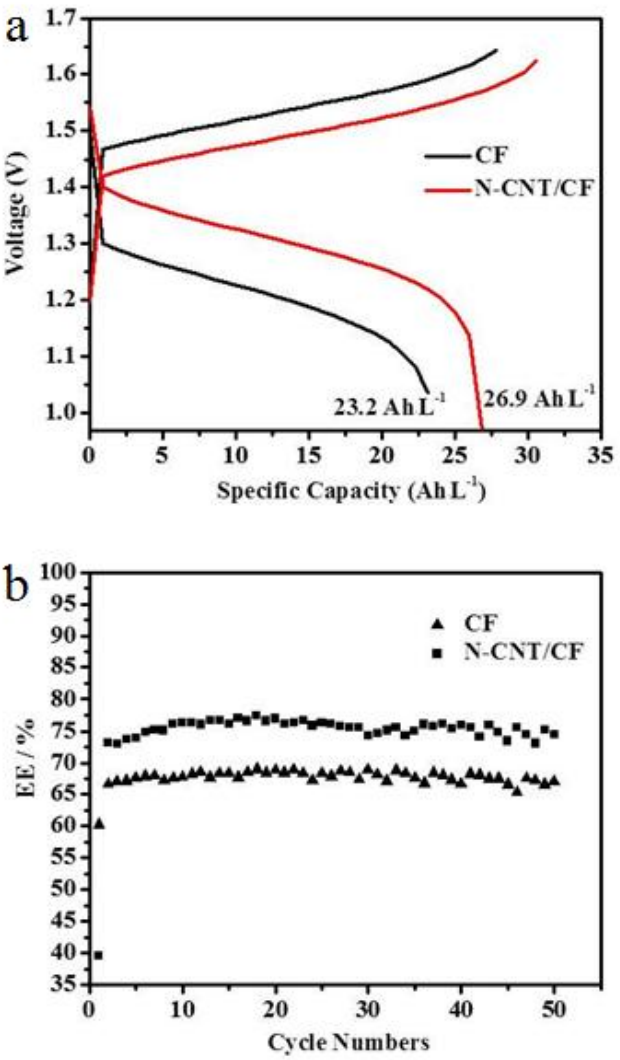

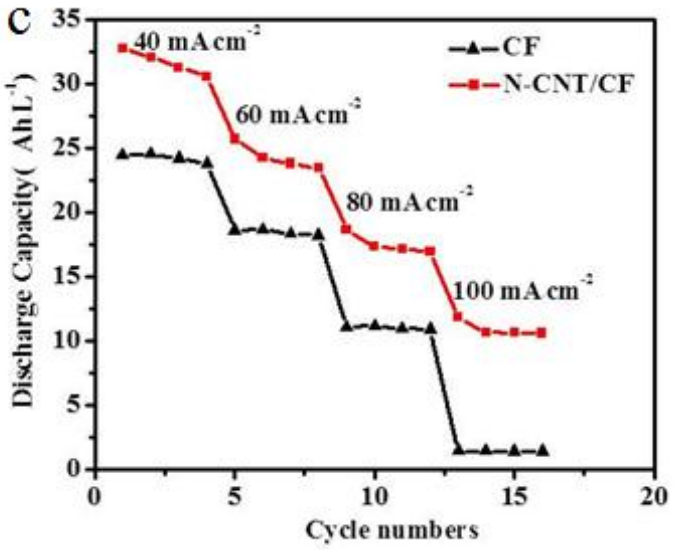


**Figure 5.** Electrochemical performance of VRB employing N-CNT/CF electrode and CF electrode in a flow single battery: (a) charge−discharge curves at 40 mA/cm$^2$. (b) cycling performance of the VRB at 40 mA/cm$^2$. (c) Rate performance at the current rate from 40 mA/cm$^2$ to 100 mA/cm$^2$.

To investigate the catalytic effect of N-CNTs on the performance of the VRB, the charge-discharge test was performed. Fig. 5a shows the voltage profile for the CF and N-CNT/CF, displaying the reduced overpotential about 44.6 mV and 97.7 mV in both charge and discharge processes. This suggests N-CNTs can provide more active sites for $VO^{2+}/VO_2^+$ redox couple and larger specific surface to increase the rate of electrons transfer, leading to a lower charge and higher discharge voltage. What's more, compared with the CF as a positive electrode, the N-CNT/CF electrode exhibited a higher specific capacity of 26.9 Ah·L$^{-1}$, owing to N-CNTs providing more active sites and promoting mass transfer rate faster. Moreover, the specific capacity is higher than the one previously reported[18]. This can be due to the incorporation of nitrogen improving the electrical conductivity of N-CNT/CF and increasing the active sites[21]. In addition, the coulomb efficiency, voltage efficiency and energy efficiency of N-CNT/CF are 88.8 %, 86.0 % and 76.3 %, respectively. Fig. 5b shows the cycling performance of the VRB with the positive electrode of N-CNT/CF and CF at the current density of 40 mA/cm$^2$. The EE value of N-CNT/CF is higher than that of CF, due to the catalytic effect of N-CNTs for $VO^{2+}/VO_2^+$ redox couple. Furthermore, the energy efficiency at the current density of 40 mA/cm$^2$ is fundamentally comparable to the one previously reported at the current density of 10 mA/cm$^2$, showing a superior cycling performance[22]. Over 50 cycles, EE value of N-CNT/CF is obviously unchanged, indicating the electrocatalytic effect of N-CNTs for $VO^{2+}/VO_2^+$ redox couple maintains good stability.To investigate the rate capability, the batteries were charged to 1.65 V and discharged to 0.8 V at a rate of 40 mA/cm$^2$ to100 mA/cm$^2$. As shown in Fig. 5c, with the increase of current density, both the discharge capacity of two samples decreased, attributing to higher overpotential at a large current density. At the current density of 100 mA/cm$^2$, the rate capability of the N-CNT/CF electrode is better comparing with that of the CF electrode, suggesting that N-CNTs can provide more active sites for $VO^{2+}/VO_2^+$ redox couple and possess high electrical conductivity, resulting in decreasing

polarization resistance. The N-CNT/CF electrode exhibits a higher rate capability at the current density of 100 mA/cm$^2$ than the CNF/CNT-700 one previously reported, owing to nitrogen incorporated improving the electrical conductivity of N-CNT/CF and increasing the active sites[18].

## 4. CONCLUSION

Nitrogen doped carbon nanotubes on carbon felt were successfully synthesized by using melamine as carbon and nitrogen source via a chemical vapor deposition method. The dispersal of N-CNTs on carbon fibers was relatively uniform and the diameter of N-CNTs ranged from 20 nm to 40 nm. The effect of N-CNTs on battery performance was also investigated. The results of the battery test showed that N-CNT/CF composite as positive electrode exhibited lower overpotential and higher efficiency at the current density of 40 mA/cm$^2$ and better rate capability from 40 mA/cm$^2$ to 100 mA/cm$^2$, due to better electronic network of N-CNTs and more active sites for $VO^{2+}/VO_2^+$ redox reaction on the surface of the N-CNTs electrode, leading to faster electron transfer rate and lower polarization. Therefore, the N-CNTs modified CF has a great application potential as a high-performance electrode for VRBs.

## References

1. W. Y. Li, J. G. Liu and C. W. Yan, *Carbon*, 49 (2011) 3463
2. B. T. Sun and M. Skyllas-Kazakos, *Electrochim. Acta*, 36 (1991) 513-517.
3. B. Sun and M. Skyllas-Kazakos, *Electrochim. Acta*, 37 (1992) 2459-2465.
4. M. S. Akhtar, Z. Y. Li, D. M. Park, D. W. Oh, D. H. Kwak and O. B. Yang, *Electrochimi. Acta*, 56 (2011) 9973–9979.
5. R. Kannan, P. Aher, T. Palaniselvam, S. Kurungot, U. Kharul and V. Pillai, *J. Phys. Chem. Lett.*, 1 (2010) 2109−2113.
6. I. Shakir, M. Shakir, S. Cherevko, C. H. Cherevko and D. J. Kang, *Electrochim. Acta*, 58 (2011) 76–80.
7. S. Mirershadi, A. Reyhani, S. Z. Mortazavi, B. Safibonab and M. K. Esfahani, *Int. J. Hydrogen Energy*, 36 (2011) 15622-15631.
8. C. Xiong, Z. D. Wei, B. S. Hu, S. G. Chen, L. Li, L. Guo, W. Ding, X. Liu, W. J. Ji and X. P. Wang, *J. Power Sources*, 215 (2012) 216-220.
9. H. Zhang, X. J. Liu, R. L. Wang, R. Mi, S. M. Li, Y. H. Cui, Y. F. Deng, J. Mei and H. Liu, *J. Power Sources*, 274 (2015) 1063-1069.
10. J. W. Jang, C. E. Lee, C. I. Oh and C. J. Lee, *J. Appl. Phys.*, 98 (2005) 074316.
11. Y. Cao, Q. Z. Jiao and Y. Zhao, *Acta Phys. -Chim. Sin.*, 25 (2009) 2383.
12. Y. Chai, Q. F. Zhang and J. L. Wu, *Carbon*, 44 (2006) 687-691.
13. S. Maldonado, S. Morin and K. Stevenson, *Carbon*, 44 (2006) 1429-1437.
14. E. G. Wang, Z. G. Guo and J. Ma, *Carbon*, 41 (2003) 1827-1831.
15. W. Ren, D. J. Li, H. Liu, R. Mi, Y. Zhang and L. Dong, *Electrochim. Acta*, 105 (2013) 75-82.
16. C.Rao, C. Cabrera and Y. Ishikawa, *J. Phys. Chem. Lett.*, 1 (2010) 2622−2627.
17. K. Gong, F. Du, Z. Xia, M. Dustock and L. Dai, *Science*, 323 (2009) 760−764.
18. M. Park, Y. J. Jung, J. Kim, H. I. Lee and J. Cho, *Nano Lett.*, 13 (2013) 4836.
19. G. J. Wei, X. Z. Fan, J. G. Liu and C. W. Yan, *J. Power Sources*, 281 (2015) 3.

20. B. Li, M. Gu, Z. Nie, Y. Shao, Q. Luo, X. Wei, X. Li, J. Xiao, C. Wang, V. Sprenkle and W. Wang, *Nano Lett.*, 13 (2013) 1330─1335.
21. Z. X. He, L. Shi, J. X. Shen, Z. He and S. Q. Liu, *Int. J. Energy Res.*, 39 (2015) 713.
22. S. Y. Wang, X. S. Zhao, T. Cochell and A. Manthiram, *J. Phys. Chem. Lett.*, 3 (2012) 2164-2167.